ISSN 1392–1320 MATERIALS SCIENCE (MEDŽIAGOTYRA). Vol. XX, No. X. 2022

A Study of Recycling Process of Cobalt-based Conversion Coating Formed on Aluminium Alloys

Di MA [1]*, Shubai LI [2], Dongmei YU [1], Bin WANG [1], Zou CHEN [1], Xiwen ZHOU [1], Zhenzhen XU [1]

[1] *School of Chemistry & Environmental Engineering, Jiangsu University of Technology, 1801 Zhongwu Rd., Changzhou, Jiangsu, 213001 China*
[2] *Department of Chemical Engineering, Changzhou Institute of Engineering Technology, 33 Gehu Middle Rd., Changzhou, Jiangsu, 213164 China*

crossref http://dx.doi.org/10.5755/j02.ms.28295

Received 13 January 2021; accepted 05 March 2021

In this study, the influence of different cyclic treatment and reuse process on the performance of the conversion film was systematically studied by electrochemical test, surface characterization and determination of cobalt ions in the conversion solution, and new technology of chemical conversion of cobalt salts in aluminum alloys were determined. Mode A indicated the practice of cyclical processing of the test object in the original conversion solution, in which components of the circulation liquid were consumed continuously. After the first cycle, the E_{corr} and R_p were – 691.8 V and 63.5 kΩ. In the later time, R_p was just about 13.0 kΩ, and the corrosion resistance of conversion film degraded progressively. Mode B represented the practice of adding to the original solution before cyclical processing of the test object, so that volume of the solution remains unchanged, and components of the circulation liquid kept increasing. R_P increased from 9.3 kΩ to the 69.9 kΩ at the beginning of the cycle, followed by a slow descent, and content of cobalt in the film was stable, also higher than that under model A. This demonstrates that mode A has high utilization of the cobalt in the conversion solution in the early recycling, whereas mode B can prolong the cyclic service life of the conversion solution in circulation. After adding oxidants, as $NaClO_3$, $NaBrO_3$, H_2O_2, NaClO, and $KMnO_4$, to the circulation liquid before recycling, the reuse and recycle ratio of cobalt reaches up to 41.3 %, and R_p can be promoted to123.2 kΩ at most. The life of the recycling was prolonged, while the costs of chemical conversion of cobalt were reduced.

Keywords: aluminum alloy, chemical conversion, cobalt, reutilization.

1. INTRODUCTION

This paper focuses on the investigation concerning the recycling process of cobalt-based conversion coatings on aluminum alloys. These intermediary layers are considered as environmentally-friendly alternatives to chromate layers, generally used to promote the adhesion for ceramic, as well as for paints and epoxy resin-based organic coatings [1 – 3].

Some authors [4, 5] consider that the application of a coating containing more than one material may allow the incorporation of different and desirable properties to the final product, such as higher thermal and mechanical stability to coatings; or an improvement in the coating adhesion; and the corrosion performance of the aluminum substrate.

The chromium-free conversion technology of aluminum alloy cobalt salt was first seen in 1994. Professor Schriever [6] prepared a conversion solution with a cobalt salt, a trivalent cobalt valence stabilizer (the ligand is ammonia water), a wetting agent, and an oxidizing agent, and the prepared conversion film has a good binding force with the organic coating.

The literature reports the importance of cobalt salt conversion in the production of both traditional and alternative single composition conversion coatings [4, 7, 8].

In this study, our goal was to stimulate the recycling process of cobalt conversion in manufacturing and to reduce the amount and environmental sensitivity of cobalt liquid waste. This is an attempt to explore potential alternatives to recycling processes to promote the commercialization of cobalt conversion.

The influence of two different cyclic reuse processes on the performance of the conversion film and adding oxidants, as $NaClO_3$, $NaBrO_3$, H_2O_2, NaClO, and $KMnO_4$, to the circulation liquid before recycling was systematically studied by electrochemical test, surface characterization and determination of cobalt ions in the conversion solution, and new technology of chemical conversion of cobalt salts in aluminum alloys was determined.

2. EXPERIMENTAL METHODS

Before chemical conversion, the pure aluminum plates were degreased with ethanol to eliminate organic impurities, etched with 1.5 mol/L sodium hydroxide to dissolve the natural aluminum oxides. The pretreated aluminum plates were performed by simple immersion into the conversion liquid.

* Corresponding author. Tel.: +86-15951207428.
E-mail address: *madi@jsut.edu.cn* (D. Ma)

The conversion liquid was allocated into two models: (Model A) The cobalt conversion liquid, which consisted of 26 g/L $Co(NO_3)_2{\cdot}6H_2O$, 1 g/L $KMnO_4$, and 30 g/L $HCOONH_4$, recycled ten times without adding other liquid. (Model B) The cobalt conversion liquid, which consisted of 26 g/L $Co(NO_3)_2{\cdot}6H_2O$, 1 g/L $KMnO_4$, and 30 g/L $HCOONH_4$, recycled ten times by adding the original conversion liquid.

The electrochemical properties of these samples were characterized by CHI 660C electrochemical system given TAFEL plots and electrochemical impedance spectroscopy (EIS). A conventional three-electrode electrochemical system was used, in which the samples as the working electrode, platinum foil as the counter electrode, and an Ag/AgCl electrode as the reference electrode. The TAFEL plots (–0.2 to 0.6 V) and EIS spectra (0.1 Hz to 100 kHz) were collected in 0.1M NaCl aqueous solution. The scan rate for CV was 0.1 Vs^{-1} and the oscillation potential for EIS was 10 mV. The microstructure of conversion coatings was characterized through Scanning Electron Microscopy (SEM) (SEM, Hitachi S-3400NII), X-ray Photoelectron Spectroscopy (XPS, Thermo Fisher Scientific, ESCALAB 250Xi).

3. RESULTS AND DISCUSSION

Fig. 1 a is representative of the Nyquist diagrams that have been obtained in this work with the conversion coatings which are directly exposed to the 5 % NaCl solution in the cyclic mode A.

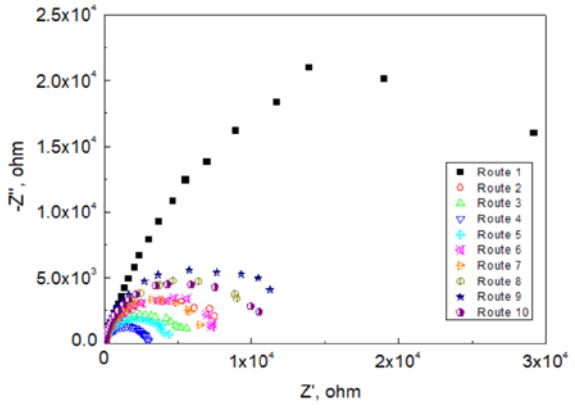

a

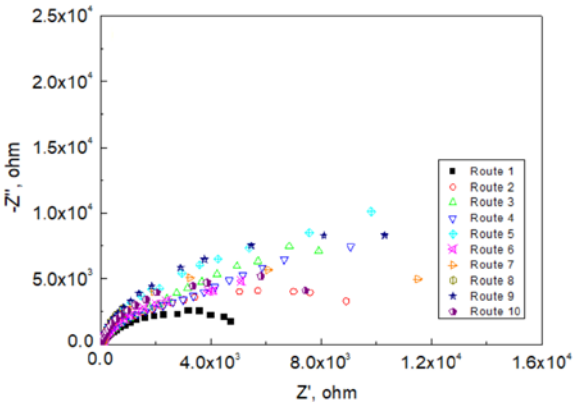

b

Fig. 1. Nyquist diagrams of cobalt conversion coatings: a – mode A; b – mode B exposure to the 5 % NaCl solution

Ten conversion coatings prepared showed a complete capacitive reactance arc in both the low-frequency region and high-frequency region in the mode A recycle. The overall change trend of the capacitive arc diameter was that the first to fourth is decreasing of the recycle, and the fifth to ninth are increasing, then fluctuate up and down within a small range and tend to stabilize. The film has good corrosion resistance characteristics is that the film has the largest capacitive reactance diameter, and high film coverage, and thicker thickness. The conversion membrane produced by the first recycle has the largest radial diameter, then the diameter of the capacitive anti-arc is reduced by about 5 times because most of the cobalt salt in the conversion solution is deposited on the surface of the substrate after the first recycle, and formed an aluminum alloys cobalt salt chemical conversion film with high coverage, thick film layer, and excellent corrosion resistance. As the number of cycles increases, the cobalt salt content in the conversion solution decrease. Accompanied by the recycle experiment and conversion fluid consumption and evaporation, the diameter of the capacitive reactance arc fluctuates within a certain range, and the variation range is small.

The impedance behavior of cobalt conversion coatings on Al alloys can be explained by the model shown in Fig. 2, where R_s, is the solution resistance between the reference electrode and the working electrode. *CPE* refers to the electric double layer and is commonly referred to as an electric double-layer capacitor. R_t is an abbreviation for the charge transfer resistance of the film layer. *W* represents the diffusion impedance response of the infinite boundary.

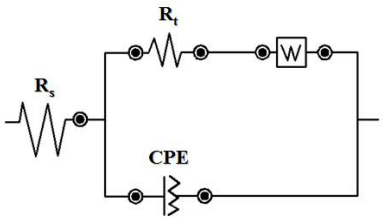

Fig. 2. The equivalent circuit used to model the impedance behavior of cobalt conversion coatings on aluminum alloys

Table 1 is the fitted parameters of the EIS of the film layer prepared in the multiple film-forming conversion liquid in the cycle mode A.

Table 1. The fitting parameters of EIS in loop mode A.

Conversion times	R_s, Ω	R_t, kΩ	Z_w, Ω	*CPE*, 10^{-6}×pF
1	13.7	78.7	2.7×10^{8}	5.1
2	14.3	8.3	1.1×10^{5}	4.6
3	14.2	5.2	9.0×10^{-4}	4.4
4	14.7	3.0	9.1×10^{9}	4.2
5	14.7	4.4	3.2×10^{-2}	4.0
6	14.7	8.1	1.2×10^{6}	4.3
7	14.8	7.4	5.7×10^{-3}	4.1
8	15.1	11.7	2.3×10^{10}	4.1
9	15.1	12.9	7.9×10^{7}	3.8
10	15.2	10.6	1.5×10^{3}	3.6

The value of the solution resistance and capacitance

changes little, the value of Z_w varies greatly, and there is no obvious regularity. The film resistance R_t is 78.7 kΩ and reaches the maximum value of mode A ten recycles after the first recycle, it can be proved that the film corrosion rate is low at this time. The R_t value is suddenly reduced to 8.3 kΩ and decreases continuously after the second recycle. At the fourth time, the minimum value is 3.0 kΩ, it can be proved that the corrosion resistance of the film is relatively poor. Then the R_t value keeps rising, reaching 10.6 kΩ after the tenth recycles, and is stable at around 10 kΩ. The overall trend of R_t is consistent with the trend of EIS changes in Fig. 1.

Fig. 1 b is representative of the Nyquist diagrams that have been obtained in this work with the conversion coatings which directly exposed to the 5 % NaCl solution in the cyclic mode B. Table 2 is the fitted parameters of the EIS of the film layer prepared in the multiple film-forming conversion liquid in the cycle mode B. The value of the solution resistance is Stable at around 15 Ω. The film resistance R_t is 6 kΩ in the first to fourth recycles, but after the fifth recycles, the R_t value rises to 16.4 kΩ and decreases to 8.6 kΩ after the sixth recycle. The R_t value rises to 24.7 kΩ in the eighth recycle, so it can be proved that the diameter of the capacitive reactance arc is gradually increasing. With the consumption of the conversion liquid, the conversion liquid is replenished to the original volume after each recycles so that the cobalt salt content in the circulating liquid continuously rises. As the number of cycles increases, the film layer is formed and the charge transfer rate is slower and the corrosion resistance is gradually increased.

Table 2. The fitting parameters of EIS in loop mode B.

Conversion times	R_s, Ω	R_t, kΩ	Z_w, Ω	*CPE*, 10^{-6}×pF
1	15.0	6.1	1.5×10^{19}	4.4
2	15.1	6.7	7.7×10^{-5}	3.8
3	15.0	6.3	2.6×10^{-5}	4.7
4	15.3	4.5	3.6×10^{-5}	3.2
5	15.5	16.4	5.6×10^{-5}	3.8
6	15.2	8.6	7.7×10^{-5}	4.4
7	15.3	13.4	1.9×10^{6}	3.9
8	15.1	24.7	20.8	4.0
9	15.7	17.1	8.8×10^{-5}	3.5
10	15.9	9.9	7.8×10^{-5}	3.6

Fig. 3 a is representative of the Tafel diagrams that have been obtained in this work with the conversion coatings which are directly exposed to the 5 % NaCl solution in the cyclic mode A. As can be seen from Fig. 3 a, the self-corrosion current density I_{corr} after the first recycle is greater than the I_{corr} obtained from the subsequent recycle. It indicates that the conversion film has the slowest corrosion rate in the electrolyte solution, the subsequent corrosion rate is accelerated, and the corrosion resistance deteriorates after the first recycle. In subsequent recycling film formation, E_{corr} is stable at around – 770 V, which is negatively shifted relative to the first recycle. It indicates that the corrosion resistance of the film decreases after the subsequent cycle, but the stability is better.

For the corrosion process generated by the electrochemical nature, according to Faraday's law, I_{corr} can be used to indicate the corrosion rate, and E_{corr} represents the motive force for controlling the corrosion reaction, the larger the I_{corr} and the more positive the E_{corr}. The corrosion rate of the film is smaller and the better the corrosion resistance. According to the theory of Stem and Geary [9], a rapid corrosion test method is known, and the value of the polarization resistance R_p is calculated according to:

$$R_p = \frac{DE}{DI} = \frac{b_a b_c}{2.303(b_a + b_c)} \frac{1}{I_{corr}} . \quad (1)$$

Corresponding to the Tafel curve corrosion resistance parameters obtained after fitting calculation are listed in Table 3. The E_{corr} after the first cycle was – 691.8 V and the R_p was 63.5 kΩ, which was significantly higher than the E_{corr} and R_p values during subsequent recycles. In the first to fourth recycles, E_{corr} gradually shifted negatively and reached the minimum value of ten times of mode A recycle, which was – 778.7 V, and the R_p was also decreasing to a minimum of 4.8 kΩ. The Polarization resistance then gradually rises to 17.8 kΩ in the fifth to ninth cycles, then fluctuates slightly at 14 kΩ and tends to stabilize.

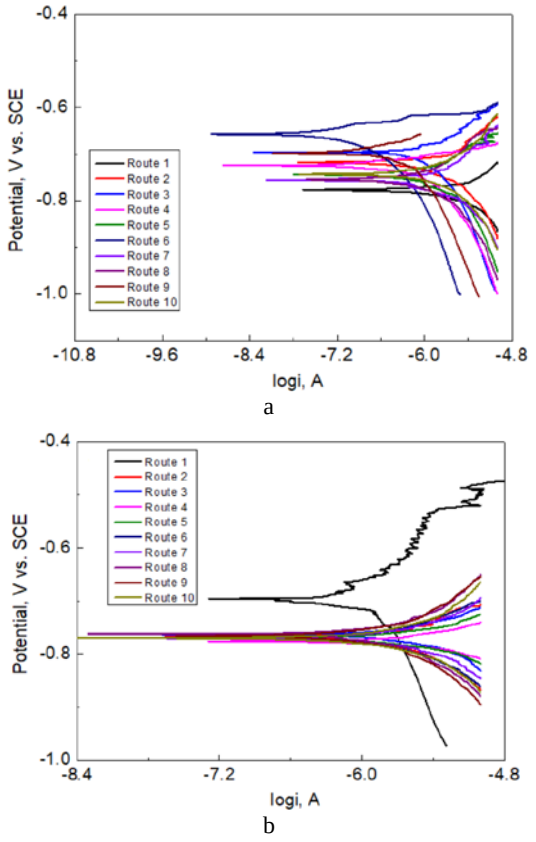

Fig. 3. Tafel diagrams of cobalt conversion coatings: a – mode A; b – mode B exposure to the 5 % NaCl solution

Fig.3 (b) is representative of the Tafel diagrams that have been obtained in this work with the conversion coatings which are directly exposed to the 5 % NaCl solution in the cyclic mode B, and the corrosion resistance parameters obtained after fitting are listed in Table 4. Tafel curve corrosion resistance parameters. In cycle mode B, the E_{corr} change of the conversion film is mainly divided into two stages: pre-cycle and post-cycle. In the early stage of recycling, E_{corr} reached – 651.7 V after the sixth cycle,

indicating that the conversion rate of the metal ions in the aluminum alloy was slower at this stage, accompanied by an increase in the cobalt salt content in the conversion solution. The anti-corrosion effect of the film is obvious, and the film has a good corrosion resistance after many times of film formation. At the end of the conversion fluid cycle, E_{corr} was reduced to – 771.3 V after the tenth cycle, indicating that as the number of cycles increased, the metal ions in the matrix continued to dissolve and accumulate in the conversion solution, causing corrosion of the conversion film and speeding up. The anodic process and the cathodic process of the electrochemical etching of the conversion film weaken the corrosion resistance of the conversion film. The change law of the Tafel curve is consistent with the trend and result of the AC impedance spectrum.

The conversion film is a closed film structure, and completely covered on the surface of the aluminum alloy, and most of the conversion film is relatively uniform. The conversion film prepared in recycle mode A is shown in Fig. 4 a and b, it can be seen from the figure that the film layer is evenly covered on the surface of the aluminum alloy, but the surface of the conversion film gradually becomes uneven. Fig. 4 c and d are a slightly porous structure in recycling mode B, and the flatness of the conversion film is higher. Combined with the results of electrochemical tests, it is known that the corrosion resistance of the film gradually decreases, and it is relatively stable in the middle of the recycle, and the fluctuation is relatively large in the later recycle.

Fig. 5 shows the XPS pattern of the conversion film prepared by the tenth film formation conversion in two different recycle modes. Fig. 5 a is the XPS general map; Fig. 5 b is the Co element narrow region map. The binding energy peaks of seven elements of O, C, Co, Al, Si, N, and S appear in the cobalt salt chemical conversion film on the surface of the aluminum alloy substrate. The atom's electron binding energy usually changes due to the chemical environment. The change in the spectrum is the shift of the peak, also called chemical shift. The chemical environment can be different from the atom. The type or amount of elements combined may be different, and the atoms may have different chemical valence states.

By consulting the XPS standard spectrum manual, the characteristic peak for O 1s is at 531.80 eV, and the characteristic peak for Al 2p is at 72.90 eV, while O 1s and Al 2p have a characteristic peak near 532.03 eV and 74.85 eV. In comparison mode A, it can be found that the binding energy of O 1s increases by 0.23 eV and 0.37 eV, respectively, and the binding energy of Al 2p increases by 1.95 eV and 2.05 eV, respectively which is consistent with the trend of mode B. Since the oxidation will increase the electron binding capacity of the inner shell, the more electrons are lost during the oxidation process, the greater the increase. From this, it can be seen that Al 2p tends to chemically shift to O 1s, and it can be concluded that Al 2p and O 1s are combined to form an oxide on the surface of the film at this time. At the binding energy of 74.30 eV ~ 74.40 eV, the main chemical state formed by the Al element which is close to the Al 2p binding energy value on the surface of the film layer is Al_2O_3.

The binding energy to the measured Co 2p is 781.83 eV, and the closest is the intrinsic oxide of $Co(OH)_2$ and cobalt. According to the narrow spectrum map of Co 2p measured by XPS, the two peaks represent the two configurations of cobalt Co 2p3 and Co 2p1, respectively, at 781.5 eV and 797.7 eV, indicating that Co exists in two modes. The standard binding energy of Co 2p3 is 778.3 eV, and the standard binding energy of Co 2p1 is 793.7 eV. The increase of binding energy indicates that oxidation occurs and electrons are lost, thus forming Co_2O_3 and Co_3O_4.

Table 3. The fitting parameters of Tafel in loop mode A

Conversion times	b_a, mV·dec^{-1}	b_c, mV·dec^{-1}	I_{corr}, μA·cm^{-2}	E_{corr}, V	R_p, kΩ
1	507.6	357.3	1.4	-691.8	63.5
2	110.5	82.8	1.7	-767.7	11.8
3	42.2	34.1	0.9	-760.6	8.7
4	18.1	34.2	1.1	-778.7	4.8
5	27.6	27.4	0.8	-770.4	7.7
6	75.4	76.1	1.3	-772.1	13.1
7	68.5	67.8	1.4	-768.9	10.3
8	130.6	87.9	1.5	-757.5	15.6
9	142.4	136.6	1.7	-768.0	17.8
10	157.7	168.6	2.6	-771.3	13.8

Table 4. The fitting parameters of Tafel in loop mode B

Conversion times	b_a, mV·dec^{-1}	b_c, mV·dec^{-1}	I_{corr}, μA·cm^{-2}	E_{corr}, V	R_p, kΩ
1	158.1	134.1	3.4	-782.2	9.3
2	73.4	45.6	0.7	-719.4	17.1
3	95.8	40.3	0.5	-693.4	23.7
4	76.9	33.7	0.3	-718.9	29.3
5	107.3	123.0	1.1	-744.3	22.4
6	373.9	37.0	0.4	-651.7	37.4
7	41.1	15.3	0.3	-752.2	19.3
8	69.6	49.3	0.5	-752.8	25.6
9	29.8	34.3	1.0	-694.4	69.9
10	93.5	88.0	1.0	-742.7	20.3

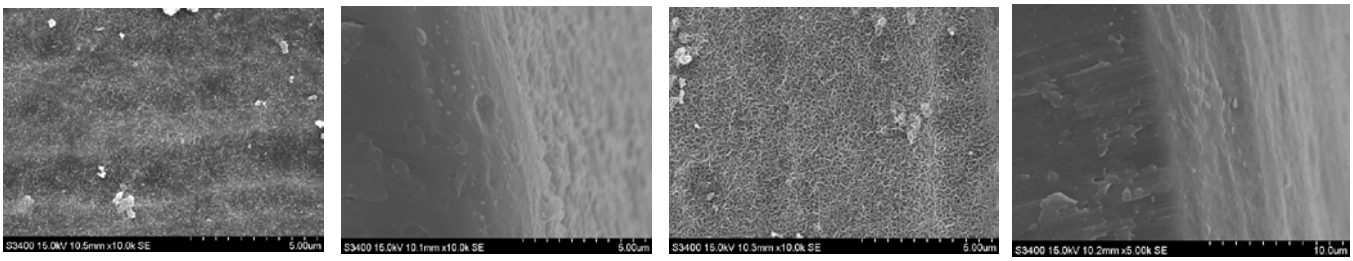

a b c d

Fig. 4. Surface and cross-section morphology of cobalt conversion coatings on aluminum alloys using: a, b – recycle mode A; c, d – mode B

The XPS narrow-area spectrum test of Co 2p shows that the total peak area of Co 2p on the aluminum sheet with a surface area of 0.25 cm^2 measured in the conversion film of mode A and mode B is 16.2 % and 3.35 %, respectively.

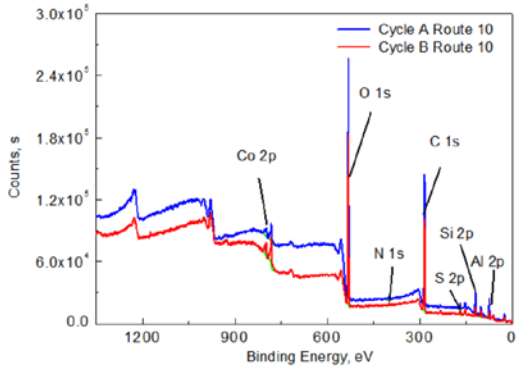

a

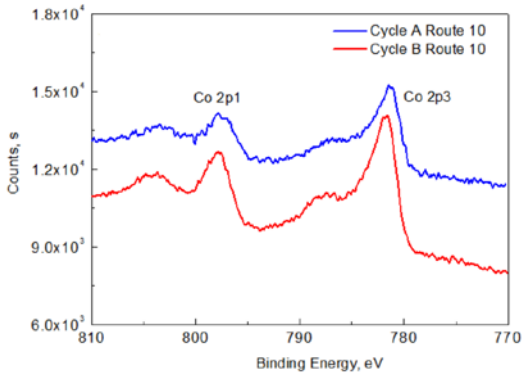

b

Fig. 5. XPS pattern of cobalt conversion coatings on aluminum alloys using: a – recycle mode A; b – mode B

The peak areas of Co 2p are 1.8×10^5 CPS.eV and 2.5×10^5 CPS.eV, respectively, indicating that the content of cobalt salt in the conversion film of the tenth cycle of mode B is higher than the tenth cycle of mode A.

With $Co(NO_3)_2\cdot6H_2O$ as the main salt, CH_5NO_2 as the ligand, and $KMnO_4$ as the oxidizer's cobalt salt conversion liquid, the thin film layer of pale gold was formed on the surface of aluminum alloys after being recycled into the film. With the increase of cycle times, the color of the conversion film gradually deepened. In the later stage of the cycle, the film is mainly composed of Co_2O_3, Co_3O_4, and Al_2O_3. When the oxidant $KMnO_4$ is added, the Co^{3+} coordination compound is generated by the reaction of the cobalt salt and the ammonium salt ligand in the conversion solution. The main reaction equation is as follows:

$$Co^{2+} + 3MnO_4^- + 7NH_4^+ = [Co(NH_3)_6]^{3+} + NO_3^- + 3MnO_2\downarrow + 4H^+ + 3H_2O \quad (2)$$

The dark brown precipitate of MnO_2 is formed by the reaction after the addition of $KMnO_4$. It is very stable at room temperature, but it can be used as a strong oxidant under acidic conditions, thus promoting the generation of Co^{2+} into high-priced cobalt ions and depositing on the surface of matrix to form conversion film:

$$2Co^{2+} + O_2 + 2H^+ = 2Co^{3+} + 2OH^- \quad (3)$$

In the mode A cycle, the conversion solution is not supplemented, so there is no supplement source of other cobalt salts or oxidants, so the corrosion resistance of the conversion film generally shows a downward trend, and the corrosion resistance is the best after the first cycle, Both *R*t and *R*p values reached the maximum, 78.7 kΩ and 63.5 kΩ, respectively, and then the corrosion resistance decreased sharply, and the *R*t and *R*p values were stable at around 15 kΩ. In the mode B cycle, the conversion raw solution is added to the original volume after each cycle, the content of cobalt salt and oxidant in the conversion liquid is gradually increased, and the corrosion resistance increases with the increase of the content of cobalt salt and oxidant in the early stage of the cycle. Gradually, the *R*t and *R*p values reached a maximum after the eighth and ninth cycles, respectively, at 27.4 kΩ and 69.9 kΩ.

Combined with the XPS test results, the cobalt salt content and the proportion in the ten-cycle mode B were higher than the mode A, and in the third and tenth cycles in the cycle mode B, the total proportion and content of the cobalt salt decreased. However, the cobalt content is slower, and it can be seen that mode A has a higher utilization rate of the cobalt salt, and the mode B can prolong the cycle life of the conversion liquid.

When the aluminum alloy is in the conversion liquid, the aluminum in the aluminum alloy is oxidized with the trivalent cobalt complex to form alumina bonded to the surface of the substrate:

$$Al + 3[Co(NH_3)_6]^{3+} = Al^{3+} + 3Co^{2+} + NH_3\uparrow; \quad (4)$$

$$2Al^{3+} + 3H_2O = Al_2O_3 + 6H^+\cdot \quad (5)$$

Besides, NH_3 generated by Eg. 2 – Eq. 6 reacts with water to form OH^-, which consumes H^+:

$$NH_3 + H_2O = OH^- + NH_4^+\cdot \quad (6)$$

The pH of the interface between the metal and the conversion solution is increased, which is favorable for the deposition of cobalt oxides in different valence states so that the ammonium salt ligand plays a role in promoting the formation of transformation.

At the same time, after the aluminum alloy is immersed in the conversion liquid, an electrochemical reaction micro-cathode reaction zone and a micro-anode reaction zone are formed in two adjacent microscopic regions on the surface of the substrate. In the micro-anode reaction zone, the metal in the matrix undergoes a dissolution reaction [10]:

$$Al \rightarrow Al^{3+} + 3e^{-}. \quad (7)$$

In the micro-cathode reaction zone, an H^+ discharge reaction occurs in the conversion solution to precipitate hydrogen gas:

$$2H^{+} + 2e^{-} \rightarrow H_2 \uparrow \cdot \quad (8)$$

The precipitation of hydrogen in the micro-cathode reaction zone causes the pH in the vicinity of the region to rise, accompanied by the dissolution of the aluminum in the micro-anode reaction region, so that the acidity at the interface between the metal and the conversion liquid gradually decreases, driving the stable three in the interface. The valence cobalt complex is converted into a cobalt oxide and deposited on the surface of the substrate to form a conversion film.

4. CONCLUSIONS

As the number of cycles increases, the content of aluminum ions in the conversion liquid increases continuously. Since an appropriate amount of aluminum ions can accelerate the formation of the conversion film and reduce the corrosion effect of chloride ions on the film layer, the film is converted in the early stage of the cycle of modes A and B. Excellent corrosion resistance, In the later stage of the cycle, both cycle modes showed a decrease in the performance of the conversion film and a certain degree of fluctuation, indicating that the stability of the film layer was poor. However, in the late stage of the mode A cycle, the content of cobalt ions and oxidants in the conversion liquid is less, which has less influence on the corrosion resistance of the film layer, while in mode B, the content of cobalt ions and oxidants is continuously increased, thereby showing that the concentration is high. The cobalt salt and the oxidant do not improve the corrosion resistance of the conversion film, but rather reduce the stability of the film layer so that the stability of mode B is lower than that of mode A at the end of the cycle.

Acknowledgments

This work was sponsored by the Natural Science Foundation of the Jiangsu Higher Education Institutions (No.17KJA610002), Jiangsu Key Research and Social Development Project (No. BE2017649), Jiangsu Overseas Research & Training Program for University Prominent Young & Middle-aged Teachers and Presidents; Changzhou Institute of technology innovation team project (2020); Jiangsu province graduate research and Practice Innovation Program (KYCX17_1876); Changzhou science and technology support plan (Social Development) (CE20195007).

REFERENCES

1. **Atzin, F. A., Miguel, D. C., Aidé, T. H.**, Cong, H., Silvia, B. S., Ana, L. O. Intensification of Electrochemical Performance of AA7075 Aluminum Alloys Using Rare Earth Functionalized Water-Based Polymer Coatings *Polymers (Basel)* 9 (5) 2017: pp 178 – 182. https://doi.org/10.3390/polym9050178
2. **Jian, S., Chang, K**. An Investigation of Mn-Ce-Based Conversion Coating on LZ91 Magnesium Alloy *International Journal of Electrochemical Science* 13 (8) 2018: pp. 8042 – 8055. https://doi.org/10.20964/2018.08.69
3. **Kosari, A., Visser, P., Tichelaar, F., Eswara, S., Mol, J. M. C.** Cross-sectional characterization of the conversion layer formed on AA2024-T3 by a lithium-leaching coating *Applied Surface Science* 512 2020: pp. 145665 – 145673. https://doi.org/10.1016/j.apsusc.2020.145665
4. **Jena, A., Munichandraiah, N., Shivashankar, S. A.** Metal-organic Chemical Vapor-deposited Cobalt Oxide Films as Negative Electrodes for Thin Film Li-ion Battery *Journal of Power Sources* 277 (1) 2015: pp. 198 – 204. https://doi.org/10.1016/j.jpowsour.2014.11.091
5. **Grolig, J. G., Froitzheim, J., Svensson, J. E.** Effect of Cerium on the Electrical Properties of a Cobalt Conversion Coating for Solid Oxide Fuel Cell Interconnects – A Study Using Impedance Spectroscopy *Electrochimica Acta* 18 (4) 2015: pp. 301 – 307. https://doi.org/10.1016/j.electacta.2015.10.111
6. **Miller, R. N.** Non-toxic Corrosion Resistant Conversion Coating for Aluminum and Aluminum.US: 5221371, 1993.
7. **Wu, B., Lu, S. X., Xu, W. G., CuI, S., Li, J. Y., Peng, F. H.** Study on Corrosion Resistance and Photocatalysis of Cobalt Superhydrophobic Coating on Aluminum Substrate *Surface and Coatings Technology* 330 (1) 2017: pp. 42 – 52. https://doi.org/10.1016/j.surfcoat.2017.09.060
8. **Ved, M. V., Sakhnenko, N. D., Karakurkchi, A. V., Myrna, T. Y.** Functional Mixed Cobalt and Aluminum Oxide Coatings for Environmental Safety *Functional Materials* 24 (2) 2017: pp. 303 – 310. https://doi.org/10.15407/fm24.02.303
9. **Stern, M., Geary, A. L.** Electrochemical Polarization: I. A Theoretical Analysis of the Shape of Polarization Curves *Journal of the Electrochemical Society* 104 (1) 1957: pp. 56 – 63.
10. **Patermarakis, G., Papandreadis N.** Effect of the Structure of Porous Anodic Al2O3 Films on the Mechanism of Their Hydration and Pore Closure During Hydrothermal Treatment *Electrochimica Acta*, 38 (10) 1993: pp. 1413 – 1420. https://doi.org/10.1016/0013-4686(93)80078-E